MRI Compatible Motion Platform

4/26/2024

Kendra Besser, Jamie Flogel, Maxwell Naslund, Amber Schneider, and Caspar Uy

Client: Mr. Jiayi Tang – UW School of Medicine and Public Health Department of Medical Physics

Advisor: Dr. James Trevathan – UW Department of Biomedical Engineering

Problem Statement

Tissue phantoms used for the testing and calibration of quantitative magnetic resonance imaging (qMRI) are typically static replicas of the human body. However, these static models fall short in accurately capturing the continuous motion due to natural physiological processes, such as respiration and digestion. To address this limitation, a specialized MRI-compatible device capable of positioning a phantom and replicating physiological movements was developed to enhance the accuracy of qMRI evaluations.

Motivation and Background

qMRI Technology

- Used to detect tissue composition, diagnose and monitor disease (steatosis), and determine drug efficiency [1][2][3]
- Phantoms are required to calibrate encoded techniques and test the accuracy/precision of imaging methods [4]
- Current Solution – Breath Holds
  - Respiratory motion produces image artifacts [5]
  - Reduced data acquisition time, typically 10 to 30s [5]
  - Unsuitable for children, severely ill, or sedated patients [6]

Competing Designs

- Vital Biomedical Technologies [7] and Quasar [8]
- Pros: user-defined trajectories, compact design
- Cons: small phantom size, $30,000+

Previous Semester

- Developed sinusoid program to control the motor
- Built preliminary prototype
- Testing showed expected displacement was not consistent with experimental displacement
- Identified Errors:
  - Faulty RPM to Voltage conversion, inaccurate clock
  - Play between gears, friction between rails and sliders

Figure 1. Motion Stage (top) [7] and Programmable Phantom (bottom) [8]

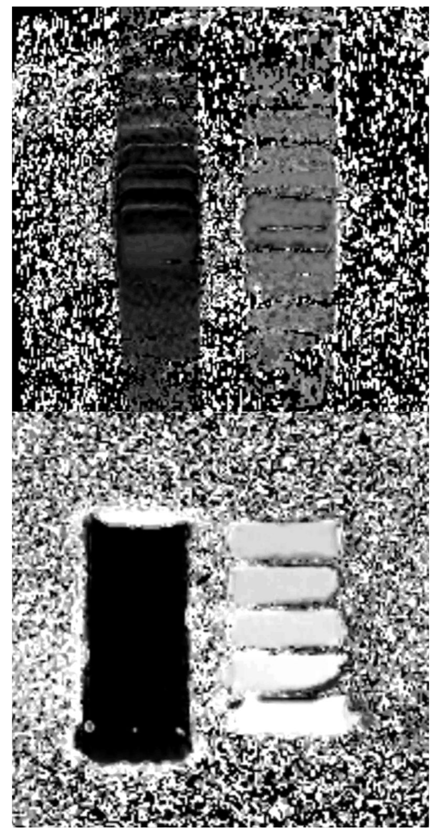

Figure 2. Non-motion robust MRI (top) and motion robust MRI (bottom)

Design Criteria

Criteria	Specification
Accuracy	Sine wave of 4-20 cycles per min with an amplitude of 1-6 cm [9]
Reliability	Sinusoidal motion within 5% deviation [10]
Accessibility	Non-complex fabrication techniques using commercially available parts
Weight	Platform to support 0-4 kg of additional weight [11]
Size	Platform larger than 25 cm by 35 cm [11]
Cost	Within budget ($1000)
Safety	MRI compatible

Final Design and Prototype Fabrication

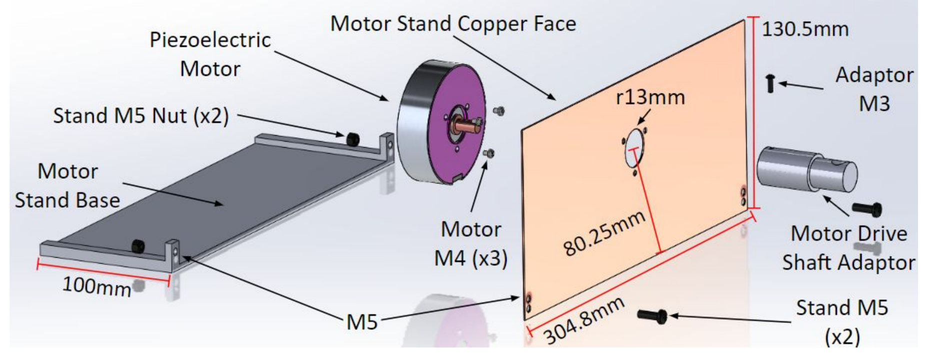

Figure 3. Motor Stand Assembly

Motor Key Features

- Microcontroller programmed to control velocity with adjustable sine wave
- Interrupts to control period using sampling rate
- Microcontroller → Motor Controller → Motor
- Fabricated in TeamLab & Makerspace

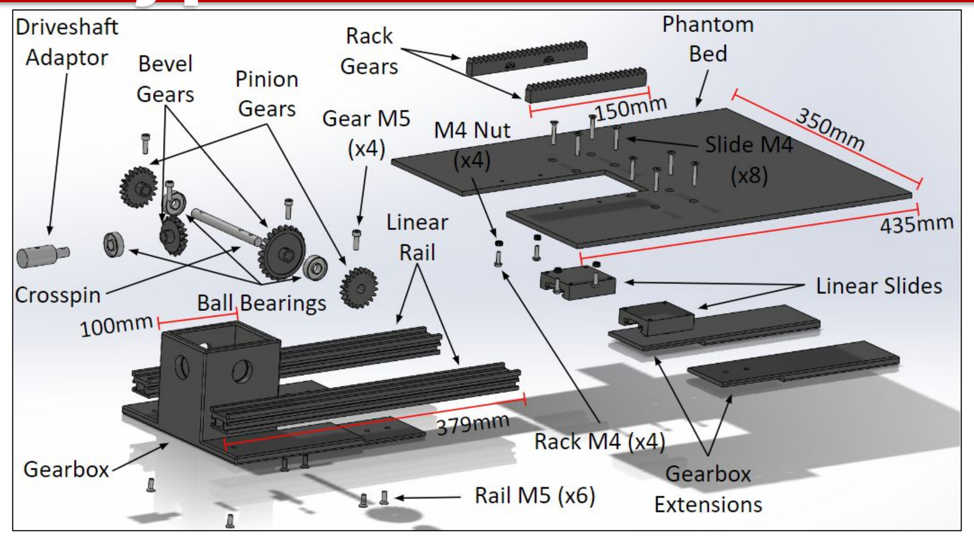

Figure 4. Gearbox and Platform Assembly

Gearbox Key Features

- Gear Ratio: 1.5:1
- Linear platform on carbon fiber rails & sliders
- Completely nonmagnetic
- Fabricated in TeamLab & Makerspace

Testing and Results

Sinusoidal Motion with Different Loads

Time between Peaks (**T = 7.50 s**)

- 0kg: 7.47 ± 0.5 s | 0.44% error
- +1.5kg: 7.60 ± 0.6 s | 1.38% error
- +3.5kg: 7.55 ± 0.5 s | 0.71% error

Peak to Peak Amplitude (**$A_{P\text{-}P}$ = 3.67 cm)**

- 0kg: 3.79 ± 0.08 cm | 3.48% error
- +1.5kg: 3.57 ± 0.06 cm | 2.51% error
- +3.5kg: 3.41 ± 0.2 cm | 7.03% error

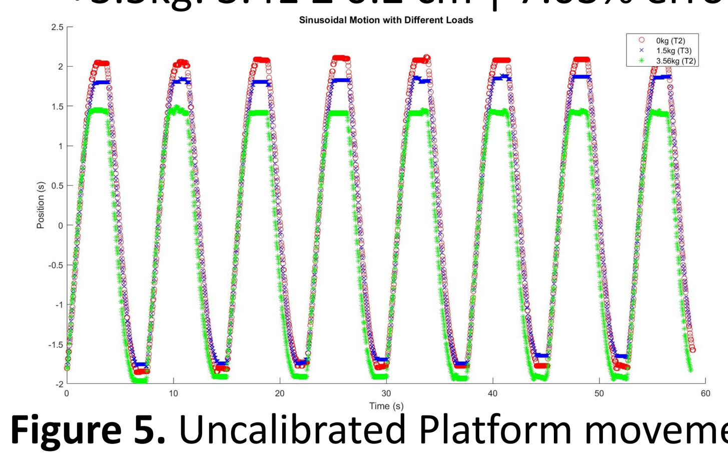

Figure 5. Uncalibrated Platform movement

RPM to Voltage Conversion Calibration

Time between Peaks (**T = 7.50 s**)

- 0kg: 7.50 ± 0.6 s | 0.06% error
- +1.5kg: 7.50 ± 0.4 s | 0.02% error

Peak to Peak Amplitude (**$A_{P\text{-}P}$ = 3.67 cm)**

- 0kg: 3.78 ± 0.05 cm | 3.12% error
- +1.5kg: 3.67 ± 0.2 cm | 0.10% error

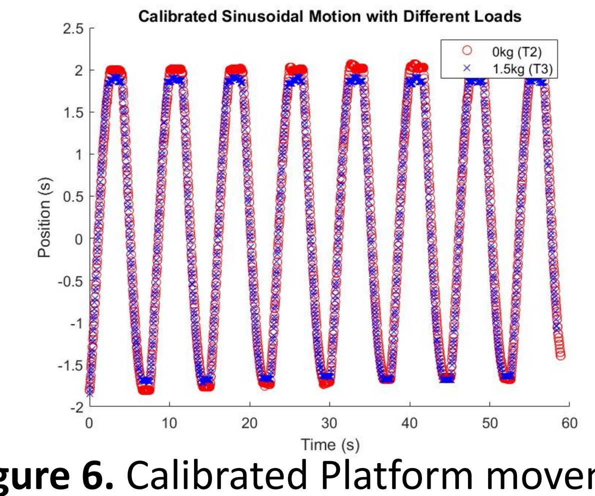

Figure 6. Calibrated Platform movement

Frequency Bounds

- 4/60Hz: 15.1 ± 0.7 s | 0.45% error
- 20/60Hz: 3.02 ± 0.2 s | 0.51% error

Amplitude Bounds

- 1cm: 0.736 ± 0.04 cm | 27.63% error
  - *Note: 2/3 trials failed*
- 6cm: 6.48 ± 0.2 cm | 6.16% error

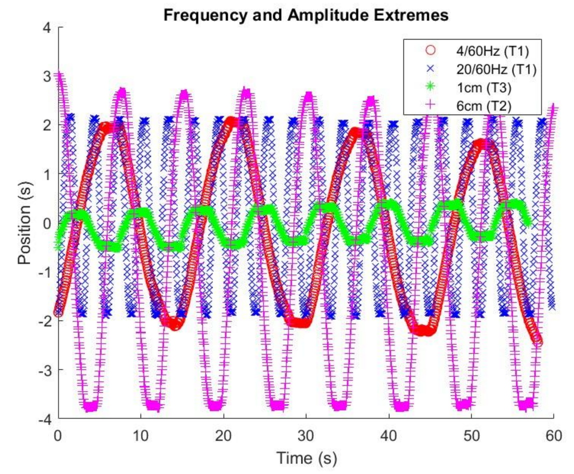

Figure 7. Extremes of Sinusoidal Motion

Discussion

Result Implications

- Low period error
- Acceptable amplitude error
- No observable relationship with weight
- Calibration improved percent error in period and amplitude
- Amplitude extremes are not within tolerance

Sources of Error

- Operating at small input range to motor driver
- Kinovea tracking software and testing setup
- Imperfect RPM to Voltage conversion
- Play between gears and driveshaft dislodgement

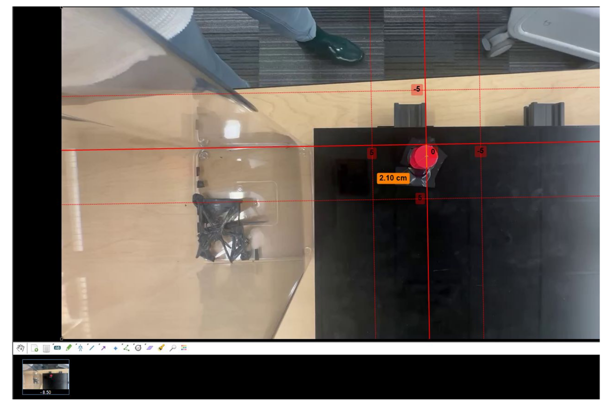

Figure 8. Kinovea tracking

Future Work

- Design Changes
  - Implement proportional control for position feedback using built in encoder
  - Optimize gear interactions and reduce friction
  - Add additional slides to reduce torque from phantom
  - Flexible coupling
  - Flip ball bearing insertion points to within gearbox
- Testing
  - Reliability testing to insure consistent waveform for 10-15 minutes
  - Compare performance with competing design
- Potential directions
  - Introduce a Low Pass Filter
  - Develop UI to change desired sinusoid
  - Retrofit design to replicate high frequency cardiac motion

Acknowledgements

The team would like to thank our advisor, Dr. James Trevathan, and our client, Mr. Jiayi Tang, for their support and guidance. Additional thanks to Dr. Samuel Hurley, Dr. Amit Nimunkar, and the rest of the BME design staff for their help in the design process.

References

[1] A. Seiler et al., "Multiparametric Quantitative MRI in Neurological Diseases," Front. Neurol., vol. 12, 2021, Accessed: Oct. 09, 2023. [Online]. Available: https://www.frontiersin.org/articles/10.3389/fneur.2021.640239

[2] K. E. Keenan et al., "Recommendations Towards Standards for Quantitative MRI (qMRI) and Outstanding Needs," J. Magn. Reson. Imaging JMRI, vol. 49, no. 7, pp. e26–e39, Jun. 2019, doi: 10.1002/jmri.26598.

[3] W. T. Reichert, "A Simple Multi-Parametric Quantitative MRI Phantom".

[4] D. A. Feinberg, N. M. Rofsky, and G. Johnson, "Multiple breath-hold averaging (mba) method for increased snr in abdominal mri," Magn. Reson. Med., vol. 34, no. 6, pp. 905–909, 1995, doi: 10.1002/mrm.1910340617.

[5] M. Kocaoglu, A. S. Pednekar, H. Wang, T. Alsaied, M. D. Taylor, and M. S. Rattan, "Breath-hold and free-breathing quantitative assessment of biventricular volume and function using compressed SENSE: a clinical validation in children and young adults," J. Cardiovasc. Magn. Reson., vol. 22, no. 1, p. 54, Jul. 2020, doi: 10.1186/s12968-020-00642-y.

[6] P. Bannas et al., "Quantitative magnetic resonance imaging of hepatic steatosis: Validation in ex vivo human livers," Hepatology, vol. 62, no. 5, pp. 1444–1455, Nov. 2015, doi: 10.1002/hep.28012.

[7] "Motion Stages Compatible with CT, MRI, PET, SPECT & Ultrasound." https://www.simutec.com/Products/motionstages.html (accessed Sep. 20, 2023).

[8] "QUASARTM MRI4D Motion Phantom," Modus Medical Devices. https://modusqa.com/products/quasar-mri4d-motion-phantom/ (accessed Sep. 20, 2023).

[9] J. Tang, J. Rice, J. Gwertzman, S. Reeder, A. Roldán-Alzate, and D. Hernando, "Development of an MR-Compatible Motion Phantom to Evaluate Motion-Robust Quantitative MRI", Accessed: Sep. 11, 2023. [Online]. Available: https://uwmadison.app.box.com/s/fp4knxj8nk4ww1j3frqtb91l75v0v2a0

[10] J. Nofiele et al., "An MRI-Compatible Platform for One-Dimensional Motion Management Studies in MRI," Magnetic resonance in medicine, vol. 76, no. 2, p. 702, Aug. 2016, doi: 10.1002/mrm.25903.

[11] "Liver Phantom — The Phantom Laboratory." https://www.phantomlab.com/liver-phantom (accessed Sep. 22, 2023).